Article

Clinical evolution of New Delhi Metallo-β-lactamase (NDM) optimizes resistance under Zn(II) deprivation

Guillermo Bahr[1,2], Luisina Vitor-Horen[1], Christopher R. Bethel[3], Robert A. Bonomo[3,4,5],

Lisandro J. González[1,2]#, Alejandro J. Vila[1,2,5]#

[1] Instituto de Biología Molecular y Celular de Rosario (IBR, CONICET-UNR), Rosario, Argentina.

[2] Área Biofísica, Facultad de Ciencias Bioquímicas y Farmacéuticas, Universidad Nacional de Rosario, Rosario, Argentina.

[3] Research Services, Louis Stokes Cleveland Department of Veterans Affairs Medical Center, Cleveland, OH 44106, United States;

[4] Departments of Medicine, Pharmacology, Molecular Biology and Microbiology, Biochemistry, Proteomics and Bioinformatics, Case Western Reserve University School of Medicine, Cleveland, OH 44106, United States;

[5] CWRU-Cleveland VAMC Center for Antimicrobial Resistance and Epidemiology, Cleveland, OH 44106, United States.

Running Title: Molecular Features in the Evolution of NDM lactamase

To whom correspondence should be addressed:

lgonzalez@ibr-conicet.gov.ar, vila@ibr-conicet.gov.ar

ABSTRACT

Carbapenem-resistant Enterobacteriaceae (CRE) are rapidly spreading and taking a staggering toll on all healthcare systems, largely due to the dissemination of genes coding for potent carbapenemases. An important family of carbapenemases are the Zn(II)-dependent β-lactamases, known as Metallo-β-lactamases (MBLs). Among them, the New-Delhi Metallo-β-lactamase (NDM) has experienced the fastest and widest geographical spread. While other clinically important MBLs are soluble periplasmic enzymes, NDM β-lactamases are lipoproteins anchored to the outer membrane in Gram-negative bacteria. This unique cellular localization endows NDM with an enhanced stability upon the Zn(II) starvation elicited by the immune system response in the sites of infection. Since the first report of NDM-1 β-lactamase, new allelic variants (16 in total) have been identified in clinical isolates, differing by a limited number of substitutions. Here we show that these variants have evolved by accumulating mutations that enhance their stability or the Zn(II) binding affinity *in vivo*, overriding the most common evolutionary pressure acting on catalytic efficiency. We identified the ubiquitous mutation M154L as responsible of improving the Zn(II) binding capabilities of the NDM variants. These results also reveal that Zn(II) deprivation imposes a strict constraint in the evolution of this MBL, overriding the most common pressures acting on catalytic performance, and shed light on possible inhibitory strategies.

INTRODUCTION

Carbapenem-resistant Enterobacteriaceae (CRE) are rapidly spreading and taking a staggering toll on all healthcare systems (1, 2), largely due to the dissemination of genes coding for potent carbapenemases (3). Metallo-β-lactamases (MBLs) are Zn(II)-dependent enzymes that represent one of the largest group of carbapenemases. MBLs are able to hydrolyze not only carbapenems, but also penicillins and cephalosporins with comparable performances (4, 5). They include the families of plasmid-encoded IMP, VIM and NDM enzymes, which have disseminated worldwide among opportunistic and pathogenic bacteria. These enzymes are not affected by the action of serine-β-lactamase inhibitors, including the newly developed avibactam, and there are not specific inhibitors for MBLs available in the clinic.

The New-Delhi Metallo-β-lactamase (NDM) has experienced the fastest and widest geographical (6, 7) spread among MBLs in recent years. The clinical success of NDM has been attributed to the fact that is a lipoprotein anchored to the outer membrane in Gram-negative bacteria (Fig. 1B) (8-10). This feature is exclusive to this enzyme in contrast to all other MBLs, which are soluble periplasmic proteins (5). We have recently suggested (9) that this cellular localization can boost the fitness of NDM-1 under physiological conditions. At the sites of infection, pathogens must face the “nutritional immunity” response by the host immune system, which involves the release of large amounts of the metal-chelating protein calprotectin. As a consequence, Zn(II) levels in the bacterial periplasm decrease, leading to accumulation of apo (non-metallated) MBLs, that

are susceptible to proteolytic degradation (9). Membrane anchoring prevents degradation of apo-NDM-1 upon this Zn(II) starvation process (9).

Since the first report of NDM-1 (11), new allelic variants (16 in total) have been identified in clinical isolates, differing by a limited number of substitutions (12). The 16 NDM variants are characterized by substitutions at a relatively small number of positions, all occurring outside the active site (Fig. 1). Residue M154 is the most frequently substituted, with M154L being the most common change (found in the single mutant NDM-4 and in six double mutants: NDM-5, NDM-7, NDM-8, NDM-12, NDM-13 and NDM-15), and one occurrence of M154V (in NDM-11). Residue D130 is replaced in 3 alleles, with substitutions D130G (NDM-8 and NDM-14) and D130N (NDM-7). Substitutions D95N and A233V are present in two alleles each, both as single variants (NDM-3 and NDM-6) and in combination with M154L (NDM-13 and NDM-15) (Fig. 1A). However, comparative studies of MBL proteins NDM 1-8 have not revealed significant differences in their resistance profiles nor in the *in vitro* activities of the purified, soluble forms of these enzymes (with truncated lipidation sites) (13). These observations cannot account for the selection of these alleles in clinical environments.

We contend that the expression of NDM variants should be evaluated in conditions as close as possible to the physiological ones: (1) in the membrane-bound form, and (2) under environmental conditions of Zn(II) deprivation (9, 14, 15). Here we examine the resistance profiles of the different NDM variants under these conditions, identify the molecular features responsible for the observed phenotypes, and demonstrate that NDM variants are evolving by enhancing their

Zn(II) binding capability *in vivo*. These results also reveal that Zn(II) deprivation has imposed a strict constraint in the evolution of this MBL, overriding the most common pressures acting on catalytic performance, and shed light on possible inhibitory strategies.

RESULTS

To compare the performance of NDM variants within a common physiological background, we expressed the *bla*$_{NDM}$ genes coding for all 16 alleles in an isogenic *E. coli* strain with their native signal peptide, targeting the variants to the outer membrane with expression levels similar to those observed in clinical strains (9, 16). To ensure homogeneous immunodetection and quantitation, all variants were expressed fused to a common C-terminal Strep-tag, which does not affect resistance (9). Expression of *bla*$_{NDM}$ alleles resulted in similar protein levels, except for NDM-10 (harboring 5 substitutions), displaying a 5-fold reduction with respect to NDM-1 (Fig. S1). In the case of NDM-2, carrying mutation P28A, 20% of the total protein was found as a soluble, non-lipidated periplasmic lactamase, indicating that mutations proximal to the lipidation site (C26) can affect membrane anchoring.

In these constructs, minimum inhibitory concentrations (MICs) of piperacillin (PIP), cefepime (FEP), cefotaxime (CTX) and imipenem (IPM) for most variants did not reveal major differences among *bla*$_{NDM}$ alleles (Table S1), except for *bla*$_{NDM-10}$. This quintuple mutant displayed significantly lower MIC values, that we attribute to the lower protein levels of this variant. Overall, these resistance profiles do not

differ from those reported for alleles *bla*$_{NDM\ 1\text{-}8}$ (13). However, the experimental conditions employed to study the resistance profile may not always reflect the actual environment that is acting in selection (17). For instance, the standard conditions used for MIC determinations involve media with high Zn(II) content that do not represent the environment at infection sites, where potent metal-sequestering proteins such as calprotectin (CP) are released by the host immune system (10, 18-21). We therefore evaluated the impact of Zn(II) deprivation in MIC values by adding the chelating agent dipicolinic acid (DPA) to the medium. It has already been shown that DPA can mimic the effect elicited by the action of CP, without being lethal for bacteria (9).

These experiments (summarized in Fig. 2) revealed that: (1) MIC values were affected by addition of DPA; and (2) the response was strongly allele-dependent. In general, the impact of Zn(II) deprivation on MIC values was noticeable at DPA levels higher than 350 µM (Fig. 2 and Table S2). Most NDM variants granted higher MIC values than NDM-1 at DPA levels beyond this value. NDM-10 was an exception, since resistance levels for this variant were drastically abolished at low concentrations of DPA. These results clearly show that the amino acid substitutions have a defined and distinct impact in the ability to endure Zn(II) starvation.

NDM variants can be classified into four groups according to the dependence of resistance on DPA concentration. *Tier 1* alleles are those displaying the highest tolerance to Zn(II) scarcity: NDM-15 (M154L A233V), NDM-13 (D95N M154L), NDM-12 (M154L G222D), NDM-8 (D130G, M154L), NDM-7

(D130N M154L), and NDM-5 (V88L M154L). *Tier 2* alleles possess greater tolerance to Zn(II) starvation than NDM-1, with MICs at least one 2-fold dilution below the lowest of *Tier 1* variants. *Tier 2* includes NDM-14 (D130G), NDM-9 (E152K), NDM-6 (A233V), NDM-4 (M154L) and NDM-3 (D95N). *Tier 3* MBLs behave similarly to NDM-1, and includes NDM-16 (R264H), NDM-11 (M154V), NDM-2 (P28A) and NDM-1. Finally, *Tier 4* contains NDM-10, the only allele that performs worse than NDM-1.

Tier 1 consists of double mutants while *Tier 2* contains only single mutants, indicating that variants with two mutations possess a higher ability to confer resistance under low Zn(II) conditions. This observation suggests that tolerance to Zn(II) starvation is selected as mutations accumulate during the evolution of NDM. Furthermore, all *Tier 1* variants possess substitution M154L, which seems crucial for adaptation to low Zn(II) availability. This enhancement can in principle be attributed to the specific presence of a leucine residue in position 154, since NDM-11 (M154V) displays a behavior similar to NDM-1 upon addition of DPA (Fig. 2).

We interrogated the role of residue 154 by performing site-saturation mutagenesis on NDM-1 at this position. MIC values of cefotaxime were within one dilution of NDM-1 for seven out of the nineteen mutants, revealing that position 154 is highly tolerant to substitutions (Table S3), in agreement with its location near the protein surface (Fig. 1B). In the presence of DPA, however, only variant M154L (NDM-4) provided higher levels of resistance than NDM-1 upon Zn(II) starvation, while all others were more susceptible (Fig. S2). The selection of replacement M154L in a position highly tolerant to mutations strongly suggests that Zn(II)

158 deprivation has exerted a significant evolutionary pressure in the natural selection
159 of NDM alleles.

160 We next aimed to characterize the molecular features giving rise to these
161 phenotypes. Zn(II) starvation elicits degradation of MBLs within the periplasmic
162 space, since the apo-enzymes (Zn(II)-free forms) are susceptible to proteolysis
163 while the metal-bound proteins are stable (9). We interrogated the *in vivo* stability
164 of NDM alleles upon Zn(II) depletion by monitoring the time evolution of the NDM
165 protein levels in *E. coli* cells after addition of DPA to the growth medium (Fig. S3).
166 Under these conditions, NDM-1 experienced >90% degradation within 60 minutes,
167 with a half-life of *ca*. 9 minutes. Degradation rates were highly variable among
168 NDM alleles, with half-lives spanning from 2 to 75 min (Fig. 3). Most variants
169 performed better or similar to NDM-1.

170 The NDM variants can be classified into four groups according to their
171 stability profiles: (1) proteins with an enhanced stability against degradation ($t_{1/2}$
172 between 75 and 53 min): NDM-15 (M154L A233V), NDM-6 (A233V) and NDM-9
173 (E152K); (2) proteins more stable than NDM-1 ($t_{1/2}$ between 20 and 17 min): NMD-
174 5 NDM-7 (D130N M154L), NDM-12 (M154L G222D) and NDM-13 (D95N M154L);
175 (3) proteins with a stability similar to NDM-1 ($t_{1/2}$ between 13 and 8 min): NDM-2
176 (P28A), NDM-3 (D130G), NDM-4 (M154L), NDM-11 (M154V) and NDM-16
177 (R264H); and (4) proteins with a markedly lower stability than NDM-1 ($t_{1/2}$ < 2 min):
178 NDM-10. Analysis of these data reveals that most double variants exhibited a
179 greater stability than NDM-1, except NDM-8 (M154L D130G) which was
180 comparable to NDM-1. Among point mutations present in NDM alleles,

substitutions A233V and E152K were shown to be stabilizing, giving rise to the only single variants displaying high stability: NDM-6 and NDM-9. The most stable NDM mutants (groups 1 and 2) outperform even SPM-1, that was previously shown to be the most stable MBL upon metal depletion under conditions similar to those reported here (Figs. S4 and S5) (9, 15).

We next analyzed possible epistatic interactions between mutations. NDM-15 (M154L A233V) shows a degradation profile similar to the single mutant NDM-6, suggesting that its high stability is mostly due to mutation A233V, while the stabilizing role of M154L is minor. A comparable stabilizing effect by mutation M154L is observed when comparing NDM-4 with NDM-1. Variant NDM-13 (D95N M154L) is more stable than the corresponding single mutants NDM-3 (D95N) and NDM-4 (M154L), and both mutations may contribute to the increased stability. NDM-8 (D130G M154L) is as stable as NDM-4, and thus D130G does not appear to significantly contribute to stability. We conclude that the effects of the different mutations on the stability are additive, with no evident epistatic interactions.

The degradation profiles upon Zn(II) starvation do not account for the resistance provided by the alleles under these conditions: NDM-4 (M154L) and NDM-11 (M154V) are degraded at a similar rate than NDM-1 (Fig. 3), but NDM-4 provides higher levels of resistance under Zn(II) deprivation (Fig. 2). Conversely, NDM-6 (A233V) and NDM-15 (M154L A233V) show similar high stabilities, but NDM-15 outperforms NDM-6 under Zn(II) starvation (Fig. 2). These observations, together with the presence of mutation M154L in all *Tier 1* mutants, reveal that

M154L enhances resistance upon Zn(II) limiting conditions without imparting protein stabilization.

Resistance at low Zn(II) levels can be optimized by two main mechanisms: (1) improved stability of the apo-proteins or (2) optimization of the Zn(II) binding affinity in the different variants, so that the accumulation of apo-proteins is minimized. Thus, we evaluated the impact of positions 154 and 233 in the metal binding affinity of variants NDM-1, NDM-4, NDM-6, NDM-11 and NDM-15, which present mutations in these positions. To assess this property, we measured the β-lactamase activity of these enzymes in spheroplasts containing the membrane-bound forms challenged with DPA. Studies on spheroplasts allow direct assessment of the enzymatic activity, being devoid of periplasmic proteases that elicit protein degradation. In all cases, we observed a decrease in activity (Fig. 4) with increasing concentrations of DPA. Immunoblotting experiments revealed similar protein levels under these conditions (Fig. S6), showing that the decrease in activity is not due to protein degradation, and therefore can be attributed to accumulation of the inactive apo-proteins generated by the chelating agent. Thus, the different behaviors of the alleles (Fig. 4) provide an estimate of the Zn(II) affinity of each variant. NDM-4 (M154L) and NDM-15 (M154L A233V) displayed the lowest susceptibility to inactivation by DPA, revealing that mutation M154L indeed increases the metal binding ability, while the stabilizing mutation A233V does not. Mutation M154V did not affect Zn(II) binding, in agreement with the resistance profile observed for NDM-11 (Fig. 2). NDM-6 presented a similar apparent affinity towards Zn(II) compared to NDM-1, confirming that mutation

226 A233V only impacts on the protein stability. This experiment allows us to propose
227 that the most frequent mutation (M154L) plays a crucial role in NDM fitness by
228 increasing the Zn(II) binding affinity.

229 Finally, we sought to directly compare the fitness of NDM alleles under
230 varying conditions of Zn(II) availability. To this end, we performed competition
231 experiments between *E. coli* cells expressing NDM-1, NDM-4, NDM-6 or NDM-15,
232 in presence of different concentrations of cefotaxime, and with or without addition
233 of metal chelators to the growth medium (Fig. 5). Both NDM-1 and single mutants
234 NDM-4 and NDM-6 displayed similar fitness in Zn(II)-rich conditions, i.e. growth
235 media not supplemented with DPA, and no allele seemed to be favored over the
236 other within the range of antibiotic concentrations tested (Fig. 5-A and B). In
237 contrast, NDM-1 and NDM-4 were selected over the double mutant NDM-15,
238 particularly at higher antibiotic concentrations (Fig. 5-C and D), in accordance with
239 their slightly higher MICs for CTX (128 vs 64-128 µg/mL). Competition experiments
240 carried out in presence of 250 µM DPA presented a radically different scenario.
241 Single mutants NDM-4 and NDM-6 were selected over NDM-1, and NDM-4 was
242 outcompeted by NDM-15. The double mutant was able to outperform NDM-1 more
243 effectively than single mutant variants, highlighting the gain in fitness due to
244 accumulation of beneficial mutations. Finally, we performed competition
245 experiments between NDM-1 and NDM-15 in the presence of calprotectin (Fig.
246 5D), obtaining results comparable to those with DPA. Thus, a similar differential
247 fitness is observed when trying to reproduce metal depletion by the host's
248 nutritional immunity response upon pathogenesis. The concentration of CP used

for the experiment (250 µg/mL) is within physiological range, since levels of up to 1000 µg/mL have been reported in infection sites (20). These competition experiments clearly reveal that alleles with better Zn(II) binding capability can outcompete NDM-1 under these conditions, even at antibiotic concentrations well below the MICs.

DISCUSSION

Assessment of the molecular features involved during the evolution of resistance requires recreating as closely as possible the environmental conditions that may have driven adaptation. For example, study of the evolution of the serine-β-lactamase TEM at sub-lethal antibiotic concentrations, such as those present in the environment, allowed an exhaustive exploration of the adaptive landscapes of this protein, leading to increased diversity of this enzyme (17). Here we consider that, during an infection, the host's immune system releases metal-chelating proteins to inhibit the growth of bacteria, which in turn compete for these essential nutrients by producing high affinity metal importers. In this context, MBLs should possess optimized Zn(II) binding capabilities to effectively mediate β-lactam resistance. In particular, clinically relevant MBLs require binding of two Zn(II) ions in the periplasm to confer resistance (22). The requirements for Zn(II) binding are stringent, since metal depletion leads to protein degradation, and loss of resistance is more dramatic. Here we show that the resistance profiles of the known NDM variants are similar when measured in Zn(II)-rich medium. Instead, significant

differences appear under Zn(II) deprivation conditions. We further show that most variants are better suited to resist these conditions than NDM-1.

Our results suggest that the pathways along which NDM alleles are currently evolving in clinical settings enhance the performance of these enzymes under low Zn(II) availability. We identified two mechanisms behind this adaptation: a) stabilization of otherwise unstable apo-enzymes, and b) enhancement of the Zn(II) affinity to maintain high levels of the active species. Substitutions A233V and E152K dramatically increase protein stability in the periplasm, while the highly frequent mutation M154L enhances metal affinity. Both mechanisms can act independently or combine without epistatic interactions to render enzymes with a higher fitness under Zn(II) deprivation conditions (NDM-15). A small group of NDM alleles (NDM-2, NDM-11 and NDM-16) did not show any advantages compared to NDM-1 in our conditions. The mutations present in these variants may be neutral, or be the result of a host specific adaptation as previously shown for SPM-1 (15), that may not be evident in *E. coli* (e.g. NDM-2 has been only detected in *Acinetobacter baumanii*) (12).

A recent work has revealed that evolution of the serine-β-lactamase TEM has been shaped by optimization of the enzymatic efficiency (23), and not by stabilization of the protein itself. Our results show that the adaptive landscape of the metallo-β-lactamase NDM has been shaped by Zn(II) deprivation conditions, leading to optimization of cofactor binding. In this regard, the identification of the ubiquitous mutation M154L as responsible of increasing the Zn(II) binding affinity in different alleles also provides a unique example of optimization of cofactor

assembly along evolution. This finding is in line with the reconstruction of the evolutionary trajectory of an *in vitro* evolved MBL, that disclosed that the Zn(II) binding affinity may be an essential feature in defining its fitness landscape (13).

Membrane localization is conserved among all NDM alleles, in contrast to serine-β-lactamases which have in most cases foregone their membrane anchoring during evolution from Penicillin Binding Proteins (PBPs) (24). This contrast may be caused by the different fitness effects of membrane anchoring in each class of enzyme, which ultimately impacts its evolutive fixation. It has been shown that TEM is functional when anchored to the outer leaflet of the inner membrane as its PBP predecessors, conferring the same resistance levels as the native soluble protein without an apparent fitness advantage (24). Meanwhile, we have previously shown that membrane anchoring of NDM-1 allows it to better tolerate Zn(II) deprivation conditions (9), as soluble variants of the enzyme are less stable and confer lower levels of resistance in low Zn(II) environments. The role of membrane anchoring in stabilization would guarantee the conservation of this characteristic. It should be noted that anchoring is but one mechanism accessible to MBLs to improve stability under these conditions, as other MBLs such as SPM-1 or NDM variants carrying the A233V or E152K mutations also possess enhanced stability against proteolytic degradation.

Despite the lack of clinically useful inhibitors, recent research has shown that MBLs may also be challenged by compounds such as Aspergillomarasmine A (AMA) (25), a Zn(II) chelator able to reverse resistance mediated by MBLs in animal models. While NDM-1 was susceptible to inactivation by this compound,

317 SPM-1 proved to be refractory (25). Our results show that NDMs are evolving
318 beyond the AMA-resistant SPM-1 MBL, indicating that tolerance to low Zn(II)
319 availability will undoubtedly allow MBLs to circumvent this type of inhibition. This
320 stresses the need to develop specifically tailored inhibitors not dependent on metal
321 chelation to combat the growing threat posed by these enzymes.

322

MATERIALS AND METHODS

Bacterial strains and reagents

Escherichia coli DH5α was used for expression of plasmid pMBLe, microbiological and biochemical studies. Unless otherwise noted, all strains were grown aerobically at 37 °C in lysogeny broth (LB) medium supplemented with gentamicin 20 µg/mL when necessary. Chemical reagents were purchased from Sigma-Aldrich, molecular biology enzymes from Promega, and primers from Invitrogen.

Construction of NDM alleles

bla$_{NDM}$ variants genes were generated from pMBLe-*bla*$_{NDM-1}$ (9), which contains the full-length *bla*$_{NDM-1}$ gene fused to a C-terminal Strep-Tag II sequence under control of an IPTG-inducible pTac promoter. Variants were constructed by site-directed mutagenesis as previously described (14) using the primers detailed in Table S4. All constructs were verified by DNA sequencing (University of Maine, USA).

Periplasm and spheroplasts preparations

Extraction of periplasmic proteins was performed as previously described (9). Briefly, 2–3 mL of *E. coli* pMBLe-*bla*$_{NDM}$ cultures were pelleted and cells were washed once with 20 mM Tris, 150 mM NaCl, pH 8.0. The washed cells were resuspended in 20 mM Tris, 0.1 mM EDTA, 20% w/v sucrose, 1 mg/mL lysozyme (from chicken egg white, Sigma-Aldrich, protein ≥90%), 0.5 mM PMSF, pH 8 (resuspension volume was normalized according to the formula V = 100 µL x OD600 x V_c, where V_c is the starting volume of culture sample), incubated with gentle agitation at 4ºC for 30 min, and finally pelleted, with the periplasmic extract

in the supernatant. The pellet consisting of spheroplasts was washed in 20 mM Tris, 20% w/v sucrose, pH 8 and resuspended in the same volume of this buffer.

MBL detection

MBL protein levels were determined by SDS-PAGE followed by Western blot with Strep-Tag® II monoclonal antibodies (at 1:1000 dilution from 200 µg/ml solution) (Novagen) and immunoglobulin G-alkaline phosphatase conjugates (at 1:3000 dilution). Protein band intensities were quantified from PVDF membranes with ImageJ software (26) and converted to relative protein amounts through a calibration curve constructed under the same experimental conditions. In all cases, Western blots with antibodies detecting GroEL were performed as loading controls.

Minimum inhibitory concentration (MIC) determinations

Cefotaxime, cefepime, piperacillin and imipenem MIC determinations were performed in LB medium using the agar macrodilution method according to CLSI guidelines (27). In order to measure the effect of Zn(II) availability on antibiotic resistance, the growth medium was supplemented with varying concentrations of the metal chelator dipicolinic acid (DPA) (Merck, >98%). In all cases, bla_{NDM} expression was induced with 100 µM IPTG.

Relative MICs as plotted in Figures 2 and Figure S2 were calculated as $(MIC_{NDM} - MIC_{control})/(MIC_{NDM + 0\ \mu M\ DPA} - MIC_{control + 0\ \mu M\ DPA})$, where MIC_{NDM} and $MIC_{control}$ refer to values measured for *E. coli* DH5α pMBLe-bla_{NDM} or pMBLe, respectively, under each set of conditions, and $MIC_{NDM + 0\mu M\ DPA}$ and $MIC_{control + 0\mu M\ DPA}$, the corresponding values in media without addition of DPA.

Effect of external Zn(II) depletion in MBL protein levels

E. coli pMBLe-bla_{NDM} cells were grown at 37ºC up to an OD_{600} of 0.4. MBL expression was induced by the addition of 100 µM IPTG, and growth was continued at 37ºC for 2 h. At this time, cultures were divided in two equal parts. One portion was treated with 500 µM DPA and the other kept as an untreated control, and both cultures were grown at 37ºC. Aliquots of DPA-treated and untreated cultures were taken at different time intervals after DPA addition: 0, 10, 30 and 60 min, and processed for immunodetection. Protein values in DPA-treated samples were reported relative to the corresponding values in untreated samples.

Competition experiments

Isogenic *E. coli* W3110(28) and *E. coli* W3110 Δ*lacZ* (29) strains were transformed with pMBLe-bla_{NDM-15}, pMBLe-bla_{NDM-6}, pMBLe-bla_{NDM-4} and pMBLe-bla_{NDM-1}. Pairs of strains expressing different NDM alelles in opposite Lac phenotype backgrounds (e.g. *E. coli* W3110 pMBLe-bla_{NDM-1} and *E. coli* W3110 Δ*lacZ* pMBLe-bla_{NDM-4}) were grown at 37ºC.

Cultures were then diluted 1/100 in fresh LB broth, and grown at 37°C to OD_{600nm} = 0.6. Equal amounts (according to OD_{600nm}) of Lac^- cells expressing one allele and Lac^+ cells producing the competing allele were mixed and diluted 1/500 in fresh LB broth, supplemented with 20 µg/mL gentamycin, 100 µM IPTG, different concentrations of cefotaxime, and either with or without addition of 250 µM DPA or 250 µg/mL CP. The greatest concentration of cefotaxime used was the maximum allowing visible growth under each condition. The competition was then carried out

by growing the cells ON at 37°C, after which ca. 100-300 cells were plated in LB-agar plates supplemented with 60 µg/mL X-Gal and 100 µM IPTG, and grown ON at 37°C. Blue and white colonies were counted to determine the proportion of Lac^+ and Lac^- cells, and thus of each variant, in the population after the competition. In order to ensure there was no effect on fitness due to the $Lac^{+/-}$ background, the experiments were repeated inverting the strains carrying each allele.

Determination of Zn(II) affinity in spheroplasts

Spheroplasts from *E. coli* cells expressing NDM variants were centrifuged and resuspended in Chelex-100-treated HEPES 10 mM, NaCl 200mM, pH 7.5. Spheroplasts were diluted 1/50 in Chelex-100-treated HEPES 10 mM, NaCl 200mM, pH 7.5 with variable amounts of DPA (0-50 µM). After incubation at 30ºC for 10 min, 550 µM imipenem was added and β-Lactamase activity measured in a JASCO V-670 spectrophotometer at 30ºC. Imipenem hydrolysis was monitored at 300 nm ($\Delta\varepsilon_{300nm}$ = –9,000 $M^{-1}cm^{-1}$).

ACKNOWLEDGEMENTS

G.B. is recipient of a doctoral fellowship from Consejo Nacional de Investigaciones Científicas y Técnicas (CONICET). A.J.V. and L.J.G. are Staff members from CONICET. This work was also supported by funds from: National Institute of Allergy and Infectious Diseases of the National Institutes of Health under award number R01AI100560. to A.J.V. and R.A.B. and Agencia Nacional de Promoción Científica y Tecnológica (ANPCyT) to A.J.V. The Cleveland Department of

Veterans Affairs, the Veterans Affairs Merit Review Program award number 1I01BX001974, and the Geriatric Research Education and Clinical Center VISN 10 also support RAB. We thank Professor Elizabeth Nolan (MIT) for providing calprotectin. The content is solely the responsibility of the authors and does not necessarily represent the official views of the National Institutes of Health or the Department of Veterans Affairs.

REFERENCES

1. Patel G, Bonomo RA. 2013. "Stormy waters ahead": global emergence of carbapenemases. Front Microbiol 4:48.

2. Nordmann P, Dortet L, Poirel L. 2012. Carbapenem resistance in Enterobacteriaceae: here is the storm! Trends Mol Med 18:263-72.

3. Prevention CfDCa. 2013. Antibiotic Resistance Threats in the United States 2013. Centers for Disease Control and Prevention, Atlanta, GA.

4. Palzkill T. 2013. Metallo-beta-lactamase structure and function. Ann N Y Acad Sci 1277:91-104.

5. Crowder MW, Spencer J, Vila AJ. 2006. Metallo-beta-lactamases: novel weaponry for antibiotic resistance in bacteria. Acc Chem Res 39:721-8.

6. Walsh TR, Weeks J, Livermore DM, Toleman MA. 2011. Dissemination of NDM-1 positive bacteria in the New Delhi environment and its implications for human health: an environmental point prevalence study. Lancet Infect Dis 11:355-62.

7. Dortet L, Poirel L, Nordmann P. 2014. Worldwide Dissemination of the NDM-Type Carbapenemases in Gram-Negative Bacteria. Biomed Res Int 2014:249856.

8. King D, Strynadka N. 2011. Crystal structure of New Delhi metallo-beta-lactamase reveals molecular basis for antibiotic resistance. Protein Sci 20:1484-91.

9. Gonzalez LJ, Bahr G, Nakashige TG, Nolan EM, Bonomo RA, Vila AJ. 2016. Membrane anchoring stabilizes and favors secretion of New Delhi metallo-beta-lactamase. Nat Chem Biol 12:516-22.

10. Gonzalez LJ, Bahr G, Vila AJ. 2016. Lipidated beta-lactamases: from bench to bedside. Future Microbiol 11:1495-1498.

11. Kumarasamy KK, Toleman MA, Walsh TR, Bagaria J, Butt F, Balakrishnan R, Chaudhary U, Doumith M, Giske CG, Irfan S, Krishnan P, Kumar AV, Maharjan S, Mushtaq S, Noorie T, Paterson DL, Pearson A, Perry C, Pike R, Rao B, Ray U, Sarma JB, Sharma M, Sheridan E, Thirunarayan MA, Turton J, Upadhyay S, Warner M, Welfare W, Livermore DM, Woodford N. 2010. Emergence of a new antibiotic resistance mechanism in India, Pakistan, and the UK: a molecular, biological, and epidemiological study. Lancet Infect Dis 10:597-602.

12. Khan AU, Maryam L, Zarrilli R. 2017. Structure, Genetics and Worldwide Spread of New Delhi Metallo-beta-lactamase (NDM): a threat to public health. BMC Microbiol 17:101.

13. Makena A, Brem J, Pfeffer I, Geffen RE, Wilkins SE, Tarhonskaya H, Flashman E, Phee LM, Wareham DW, Schofield CJ. 2015. Biochemical characterization of New Delhi metallo-beta-lactamase variants reveals differences in protein stability. J Antimicrob Chemother 70:463-9.

464 14. Meini MR, Tomatis PE, Weinreich DM, Vila AJ. 2015. Quantitative
465 Description of a Protein Fitness Landscape Based on Molecular Features. Mol Biol
466 Evol 32:1774-87.
467 15. Gonzalez LJ, Moreno DM, Bonomo RA, Vila AJ. 2014. Host-specific
468 enzyme-substrate interactions in SPM-1 metallo-beta-lactamase are modulated by
469 second sphere residues. PLoS Pathog 10:e1003817.
470 16. Pasteran F, Gonzalez LJ, Albornoz E, Bahr G, Vila AJ, Corso A. 2016.
471 Triton Hodge Test: Improved Protocol for Modified Hodge Test for Enhanced
472 Detection of NDM and Other Carbapenemase Producers. J Clin Microbiol 54:640-
473 9.
474 17. Mira PM, Meza JC, Nandipati A, Barlow M. 2015. Adaptive Landscapes of
475 Resistance Genes Change as Antibiotic Concentrations Change. Mol Biol Evol
476 32:2707-15.
477 18. Brophy MB, Hayden JA, Nolan EM. 2012. Calcium ion gradients modulate
478 the zinc affinity and antibacterial activity of human calprotectin. J Am Chem Soc
479 134:18089-100.
480 19. Cerasi M, Ammendola S, Battistoni A. 2013. Competition for zinc binding in
481 the host-pathogen interaction. Front Cell Infect Microbiol 3:108.
482 20. Corbin BD, Seeley EH, Raab A, Feldmann J, Miller MR, Torres VJ,
483 Anderson KL, Dattilo BM, Dunman PM, Gerads R, Caprioli RM, Nacken W, Chazin
484 WJ, Skaar EP. 2008. Metal chelation and inhibition of bacterial growth in tissue
485 abscesses. Science 319:962-5.
486 21. Capdevila DA, Wang J, Giedroc DP. 2016. Bacterial Strategies to Maintain
487 Zinc Metallostasis at the Host-Pathogen Interface. J Biol Chem 291:20858-20868.

488 22. Gonzalez JM, Meini MR, Tomatis PE, Medrano Martin FJ, Cricco JA, Vila
489 AJ. 2012. Metallo-beta-lactamases withstand low Zn(II) conditions by tuning metal-
490 ligand interactions. Nat Chem Biol 8:698-700.
491 23. Knies JL, Cai F, Weinreich DM. 2017. Enzyme Efficiency but Not
492 Thermostability Drives Cefotaxime Resistance Evolution in TEM-1 beta-
493 Lactamase. Mol Biol Evol 34:1040-1054.
494 24. Suvorov M, Vakulenko SB, Mobashery S. 2007. Cytoplasmic-membrane
495 anchoring of a class A beta-lactamase and its capacity in manifesting antibiotic
496 resistance. Antimicrob Agents Chemother 51:2937-42.
497 25. King AM, Reid-Yu SA, Wang W, King DT, De Pascale G, Strynadka NC,
498 Walsh TR, Coombes BK, Wright GD. 2014. Aspergillomarasmine A overcomes
499 metallo-beta-lactamase antibiotic resistance. Nature 510:503-6.
500 26. Schneider CA, Rasband WS, Eliceiri KW. 2012. NIH Image to ImageJ: 25
501 years of image analysis. Nat Methods 9:671-5.
502 27. Institute CLS. 2012. Methods for Dilution Antimicrobial Susceptibility Tests
503 for Bacteria That Grow Aerobically; Approved Standard - Ninth Edition. CLSI
504 Document M07-A9. Clinical Laboratory Standards Institute, Wayne, PA.
505 28. Bachmann BJ. 1972. Pedigrees of some mutant strains of Escherichia coli
506 K-12. Bacteriol Rev 36:525-57.
507 29. Humbert MV, Rasia RM, Checa SK, Soncini FC. 2013. Protein signatures
508 that promote operator selectivity among paralog MerR monovalent metal ion
509 regulators. J Biol Chem 288:20510-9.

510

511

512

513 **FIGURE LEGENDS**

514 **Figure 1. NDM alleles possess a limited number of substitutions located**
515 **outside the active site. A**, NDM variants and their corresponding mutations with
516 respect to NDM-1. Substitutions occurring in two or more alleles are indicated in
517 bold. **B**, Diagram showing the cellular localization of NDM-1 within the inner leaflet
518 of the outer membrane in Gram-negative bacteria and crystal structure of NDM-1
519 (PDB: 4EYL), displaying the residues mutated in clinical alleles (spheres). Spheres
520 are colored with a gradient from white to black according to increasing frequency of
521 mutation at that position among alleles. Active site Zn(II) ions are indicated as
522 green spheres, and residues acting as metal ligands are displayed as sticks.

523

524 **Figure 2. NDM alleles display an increased tolerance to Zn(II) starvation with**
525 **respect to NDM-1.** Cefotaxime MICs for *E. coli* DH5α cells expressing different
526 NDM alleles in growth medium supplemented with the indicated concentrations of
527 DPA, relative to the MIC in 0 μM of DPA. Data corresponds to three independent
528 experiments, and is presented as mean ± s.e.m.

529

530 **Figure 3. Clinical NDM variants possess enhanced *in vivo* stability upon**
531 **Zn(II) starvation. A**, MBL protein levels for NDM alleles in whole *E. coli* cells
532 quantified from western blots (Figure S3) as a function of time after addition of 500
533 μM DPA, normalized to control samples not treated with DPA. Data are presented
534 as percentage of initial protein remaining after treatment with DPA, and correspond

535 to mean ± s.e.m. of three independent experiments. Data points for each allele
536 were fitted to a first-order exponential decay, indicated as continuous curves. **B**,
537 Half-lives for NDM alleles, obtained from exponential decay fit of data in panel **A**.

538

539 **Figure 4. Substitution M154L leads to an increased Zn(II) binding affinity.**
540 Relative β-lactamase activity of spheroplasts from *E.coli* cells expressing NDM
541 alleles, after incubation for 10 min at 30ºC with different concentrations of DPA.
542 Values are presented as relative to activity at 0 µM DPA. Data corresponds to
543 three independent experiments, and is plotted as mean ± s.e.m.

544

545 **Figure 5. NDM alleles outcompete NDM-1 under Zn(II) limiting conditions.**
546 Competition experiments between *E. coli* W3110 cells expressing NDM alleles in
547 presence of increasing concentrations of cefotaxime, in growth media with and
548 without supplementation with metal chelators. **A)** NDM-1 vs NDM-4. **B)** NDM-1 vs
549 NDM-6. **C)** NDM-4 vs NDM-15. **D)** NDM-1 vs NDM-15. Data are presented as
550 mean ± s.e.m. of two independent determinations inverting the Lac+/Lac-
551 background of the strain carrying each allele.

552

A

ALLELE	MUTATIONS
NDM-1	-
NDM-2	P28A
NDM-3	**D95N**
NDM-4	**M154L**
NDM-5	V88L, **M154L**
NDM-6	**A233V**
NDM-7	**D130N**, **M154L**
NDM-8	**D130G**, **M154L**
NDM-9	E152K
NDM-10	R32S, G36D, G69S, A74T, G200R
NDM-11	**M154V**
NDM-12	**M154L**, G222D
NDM-13	**D95N**, **M154L**
NDM-14	**D130G**
NDM-15	**M154L**, A233V
NDM-16	R264H

B

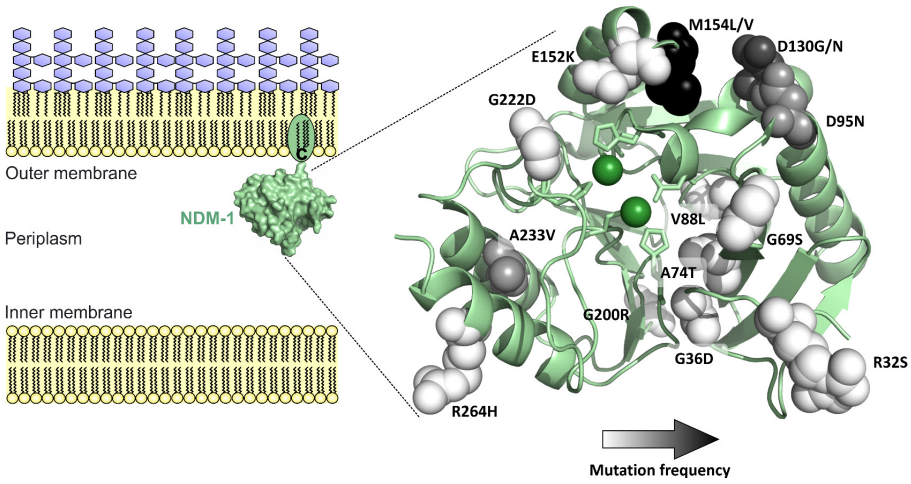

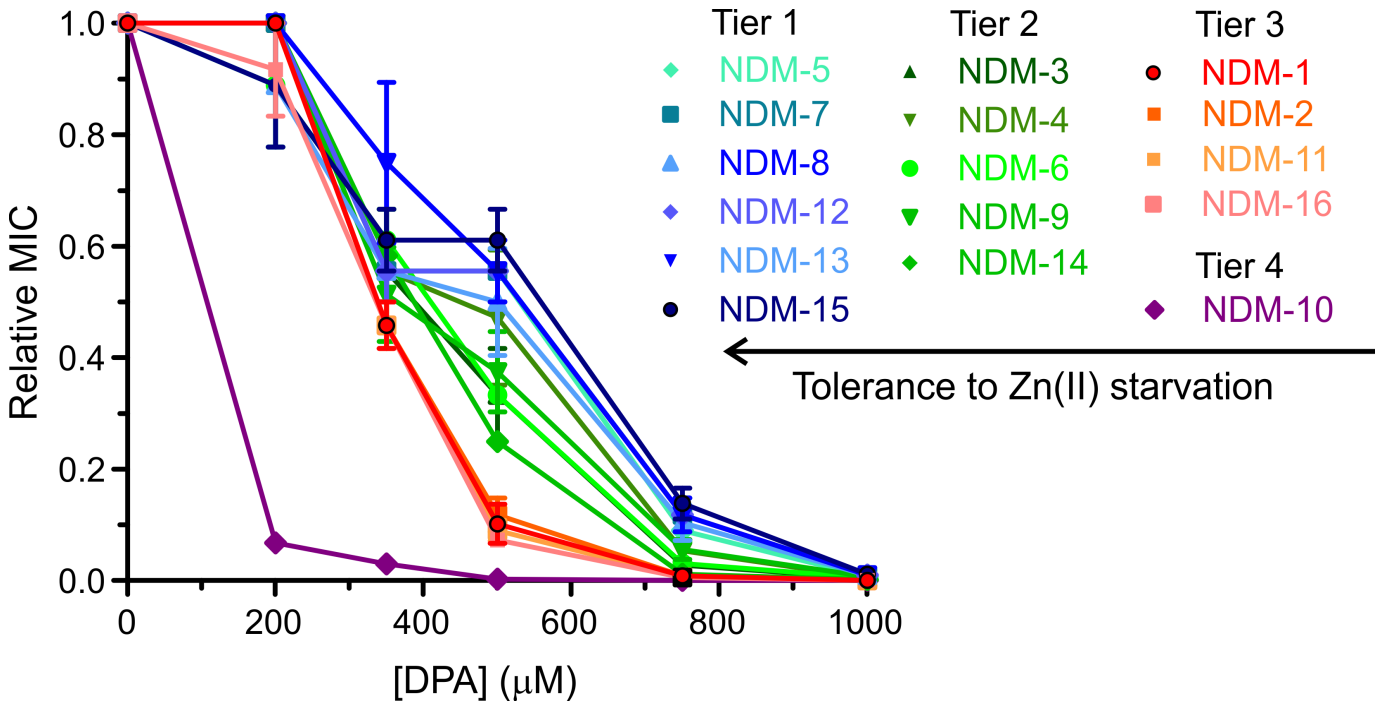

A

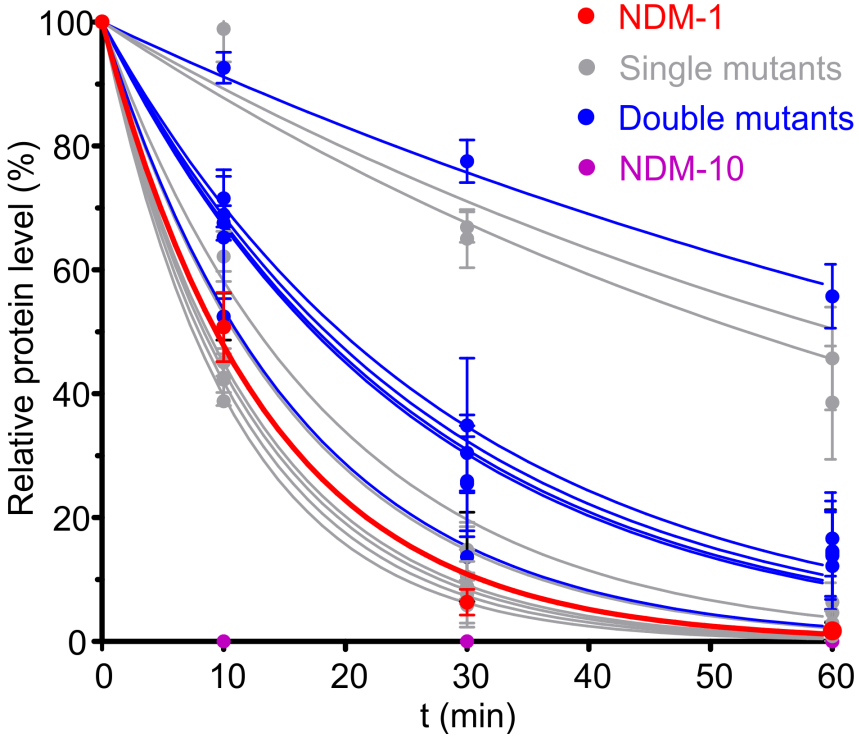

B

Allele	$t_{1/2}$ (min)
NDM-1	9
NDM-2	8
NDM-3	13
NDM-4	11
NDM-5	20
NDM-6	61
NDM-7	18
NDM-8	11
NDM-9	53
NDM-10	<2
NDM-11	8
NDM-12	17
NDM-13	18
NDM-14	8
NDM-15	75
NDM-16	9

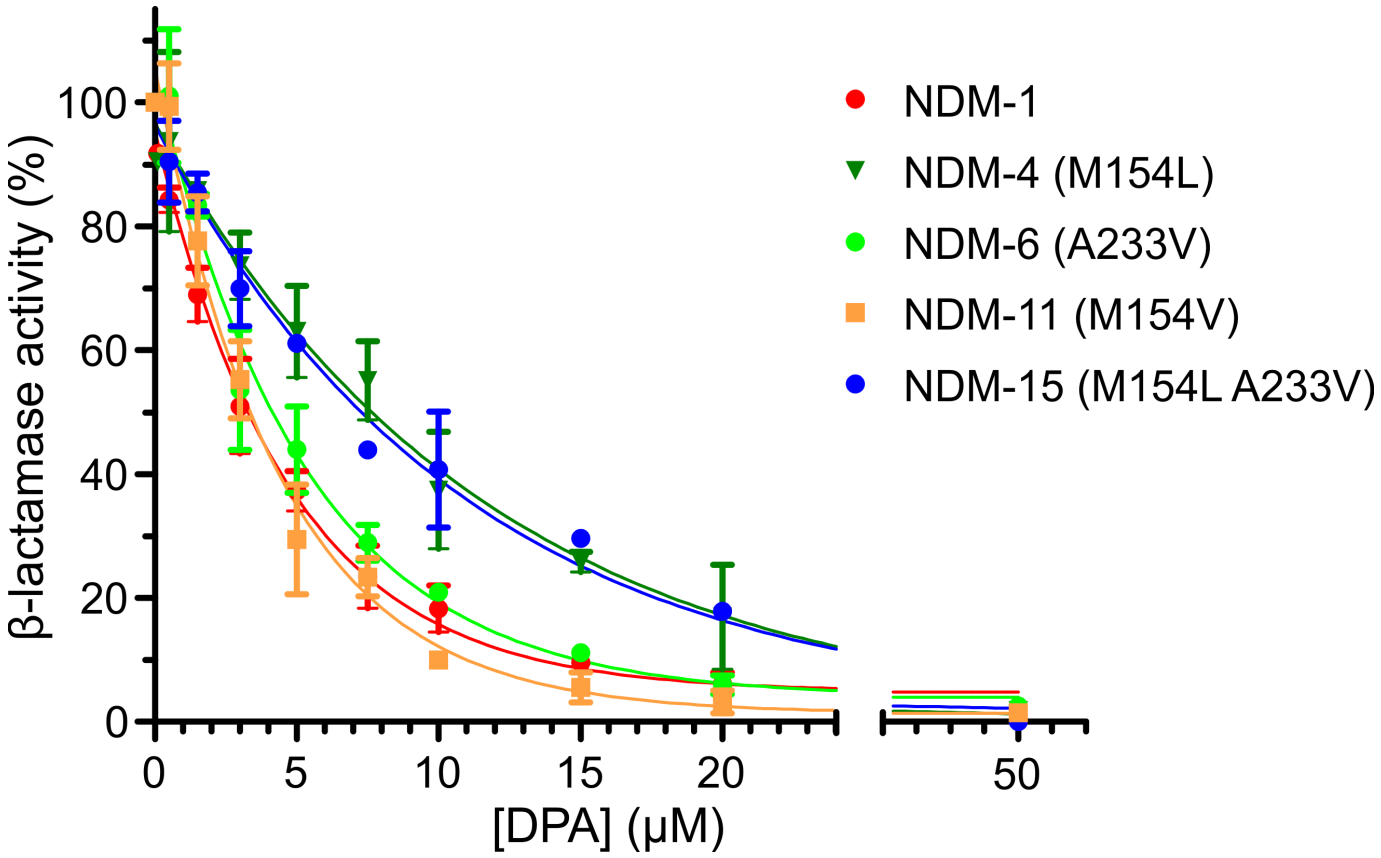

A

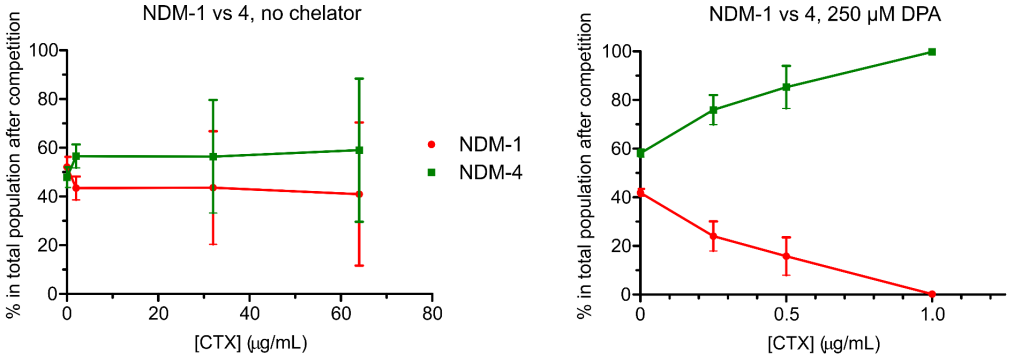

B

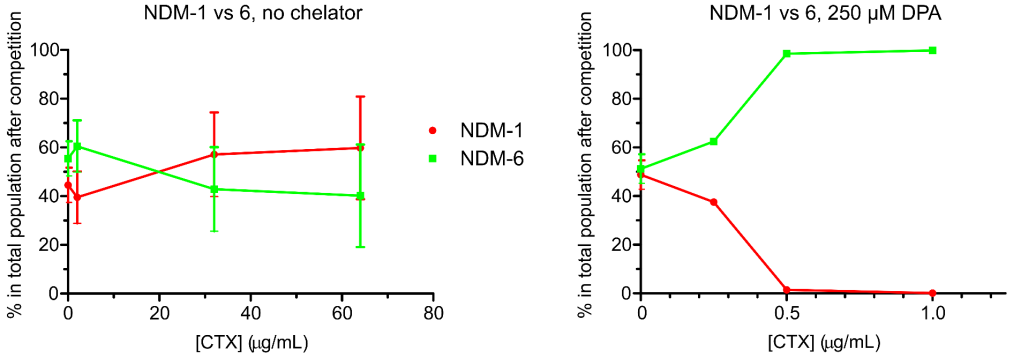

C

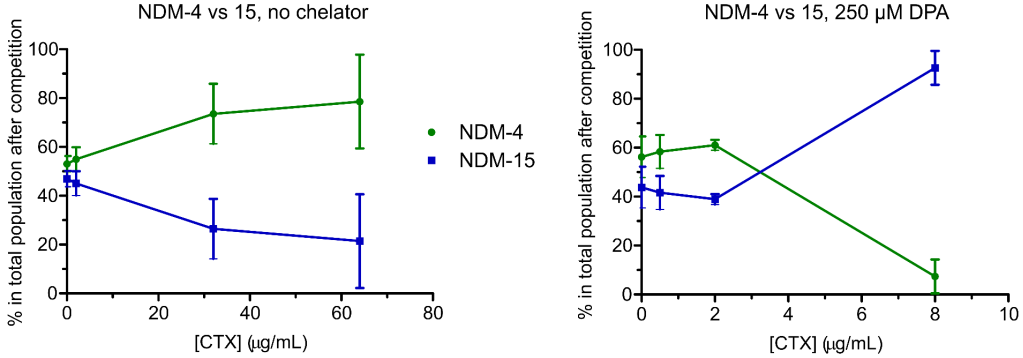

D